Optical Tomographic Imaging of Small Animals

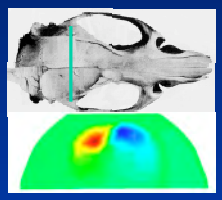
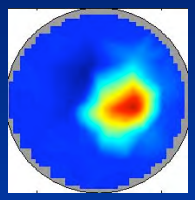


Andreas H. Hielscher, Ph.D.

Columbia University, New York City
Dept. of Biomedical Engineering
Dept. of Radiology

Overview

- **Introduction**
  - X-Ray Tomography vs Optical Tomography
- **Model-based iterative image reconstruction**
  - Basic concepts and mathematical background
- **Instrumentation**
  - General optical imaging modalities
  - Dynamic optical tomography system
- **Applications**
  - Brain Imaging
  - Tumor Imaging
  - Fluorescence Imaging

Overview

- **Introduction**
  - X-Ray Tomography vs Optical Tomography
- **Model-based iterative image reconstruction**
  - Basic concepts and mathematical background
- **Instrumentation**
  - General optical imaging modalities
  - Dynamic optical tomography system
- **Applications**
  - Brain Imaging
  - Tumor Imaging
  - Fluorescence Imaging

X-Ray Imaging

Uses X-rays to generate shadowgrams $M(\varphi,\xi)$.

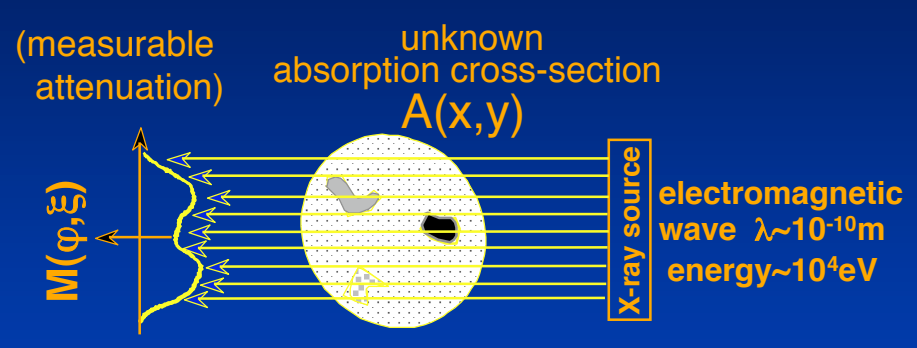

Energy propagates on straight lines through medium

X-Ray Shadowgram

X-Ray Tomography

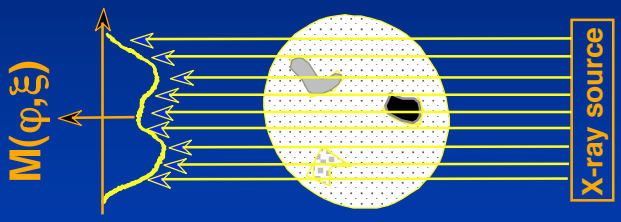

X-Ray Tomography

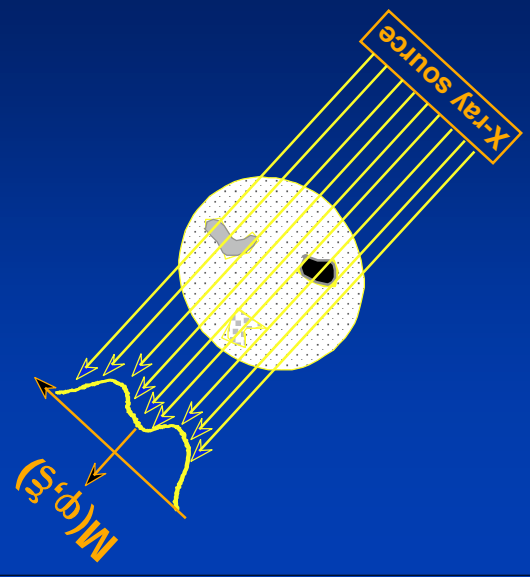

X-Ray Tomography

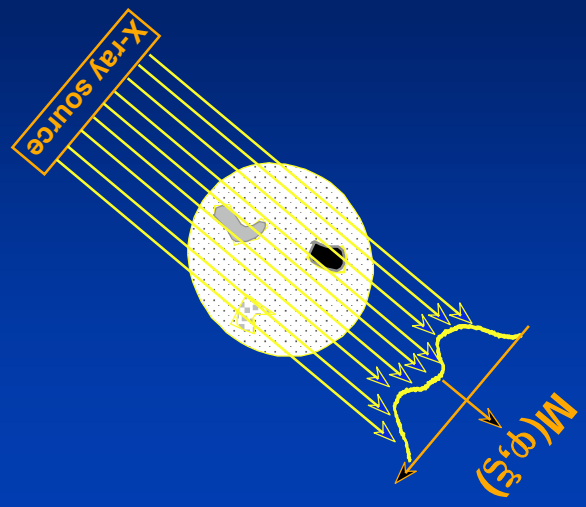

X-Ray Tomography

unknown
absorption cross-section
A(x,y)

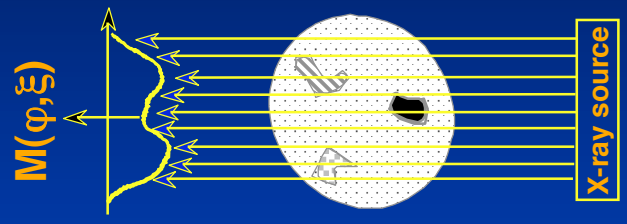

=>Simple image reconstruction scheme: backprojection of M on lines of transmission. (Inverse Radon Transform)

2D Scan of Head

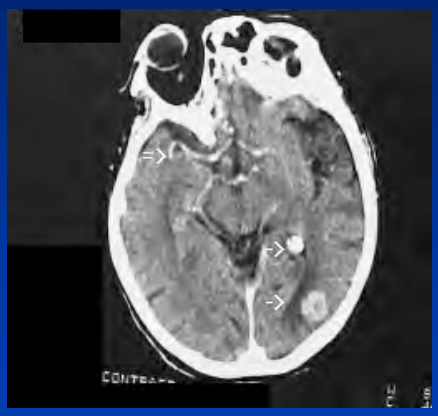

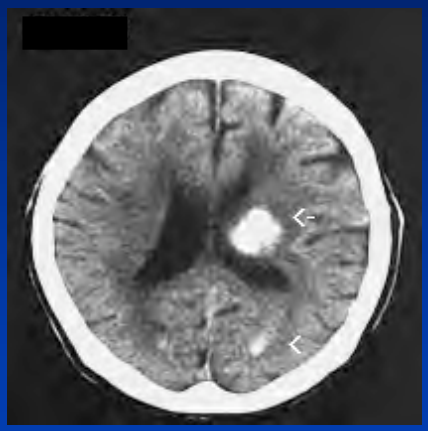

Optical Imaging

Uses near-infrared light (700< λ<900nm)

A(x,y) {unknown absorption & scattering profile}

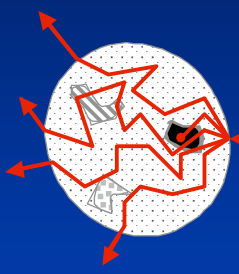

light source

EM - wave
$\lambda \sim 800 \cdot 10^{-9}$m
energy ~ 1 eV

Energy does not propagate on straight line between source and detector (light is strongly scattered)

Optical Shadowgram

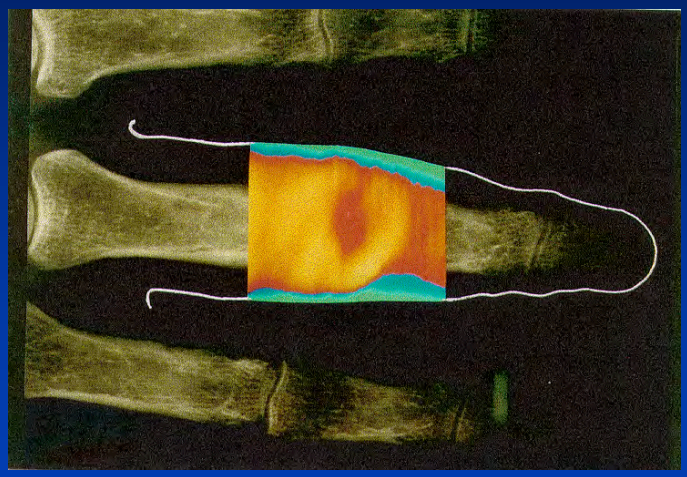

Optical Tomography

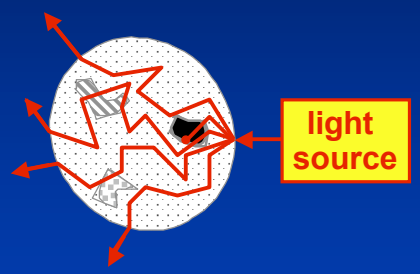

Optical Tomography

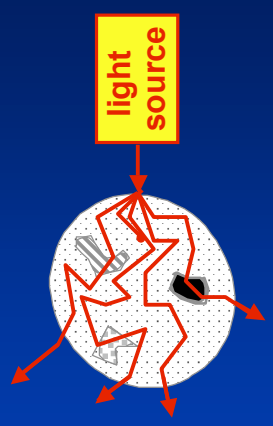

Optical Tomography

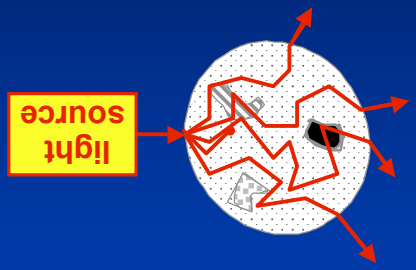

Optical Tomography

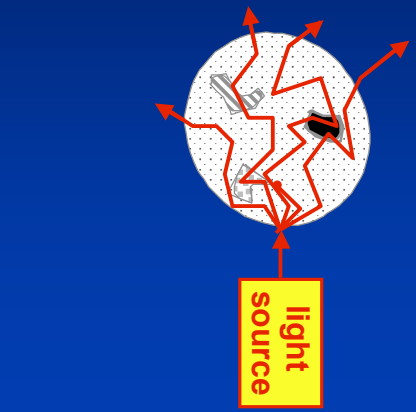

Optical Imaging

Uses near-infrared light (700< λ<900nm)

A(x,y) {unknown absorption & scattering profile}

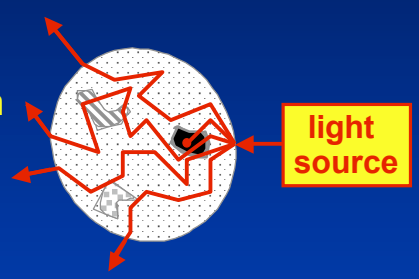

EM - wave
$\lambda \sim 800 \cdot 10^{-9}$m
energy ~ 1 eV

How to reconstruct cross-sectional images A(x,y) from measurement on surface?
(Inverse Problem)

Overview

- **Introduction**
  - X-Ray Tomography vs Optical Tomography
- **Model-based iterative image reconstruction**
  - Basic concepts and mathematical background
- **Instrumentation**
  - General optical imaging modalities
  - Dynamic optical tomography system
- **Applications**
  - Brain Imaging
  - Tumor Imaging
  - Fluorescence Imaging

Model-Based Iterative Image Reconstruction

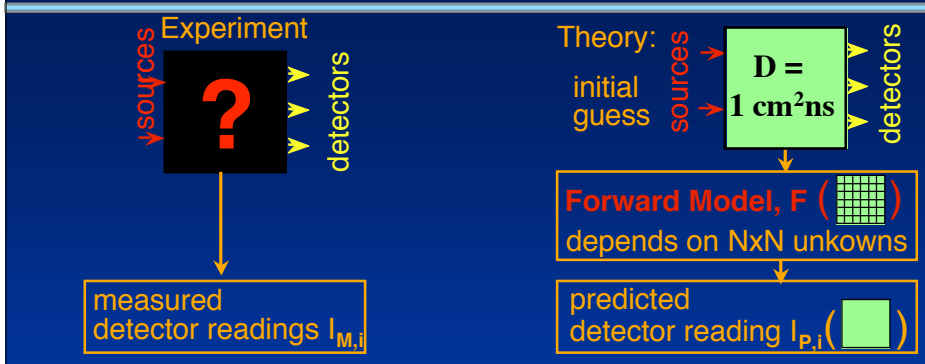

Forward Model I

3D-Time-Resolved Diffusion Equation

$$\frac{\partial U}{\partial t} = \frac{\partial}{\partial x} D \frac{\partial U}{\partial x} + \frac{\partial}{\partial y} D \frac{\partial U}{\partial y} + \frac{\partial}{\partial z} D \frac{\partial U}{\partial z} - c\mu_a U + S$$

with c := speed of light in medium, S = Source,

and **diffusion coefficient** : $D = c / (3 [\mu_a + \mu_{s'}])$

with μ_a = absorption coefficient and

$\mu_{s'}$ = reduced scattering coefficient .

Diffusion vs Transport Model

diffusion equation

approximation

$$\frac{\partial U}{\partial t} = \nabla c/(3\mu_a+3\mu_s')\,\nabla U - c\mu_a U + S$$

discretize into N spacial variables
leads to N finite-difference equations

equation of radiative transport

$$\partial\Psi/c\partial t = S - \Omega\nabla\Psi - (\mu_a+\mu_s)\Psi + \int_{4\pi}\Psi(\Omega')\,p(\Omega*\Omega')\,d\Omega'$$

with $U = \int_{4\pi}\Psi(\Omega')\,d\Omega'$ and $\mu_s' = (1-g)\,\mu_s$

discretization into N spacial and A angular variables
leads to N x A coupled finite-difference equations

slower by factor ~A

Limits of Diffusion Model

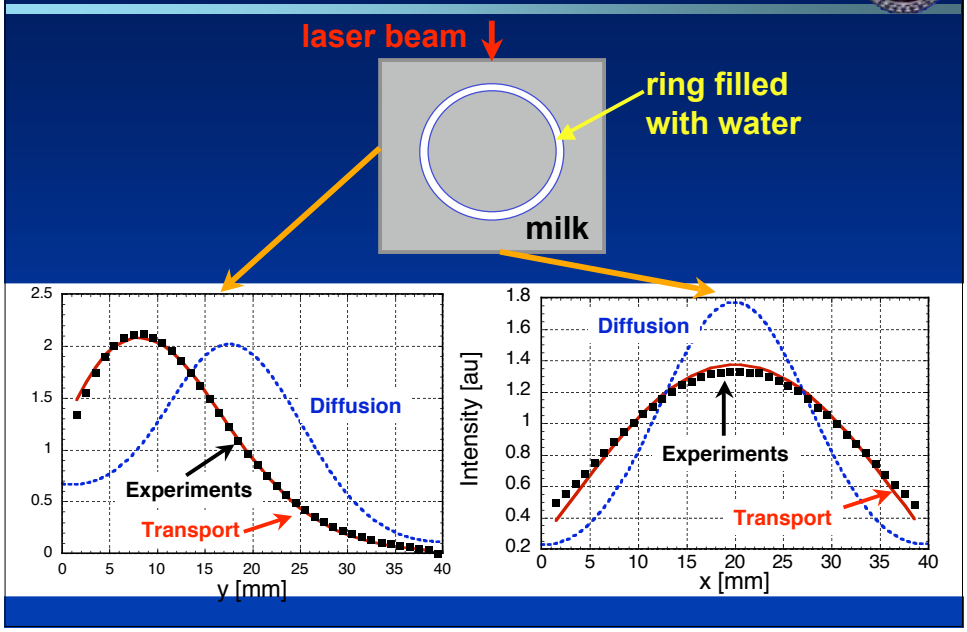

Forward Model applied to Mouse Head

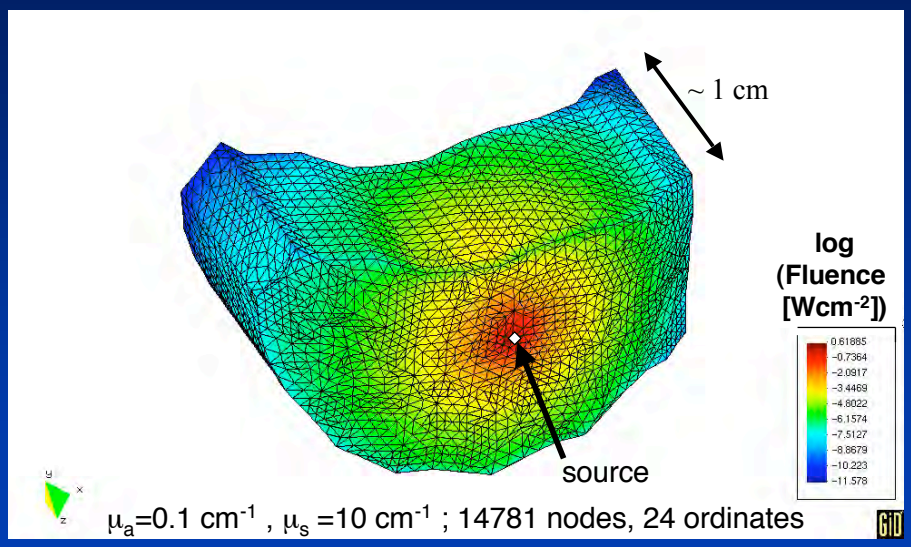

μ_a=0.1 cm^{-1} , μ_s =10 cm^{-1} ; 14781 nodes, 24 ordinates

Model-Based Iterative Image Reconstruction

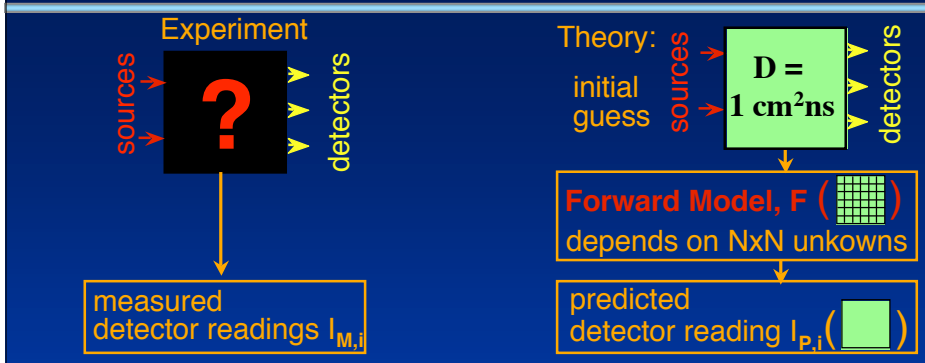

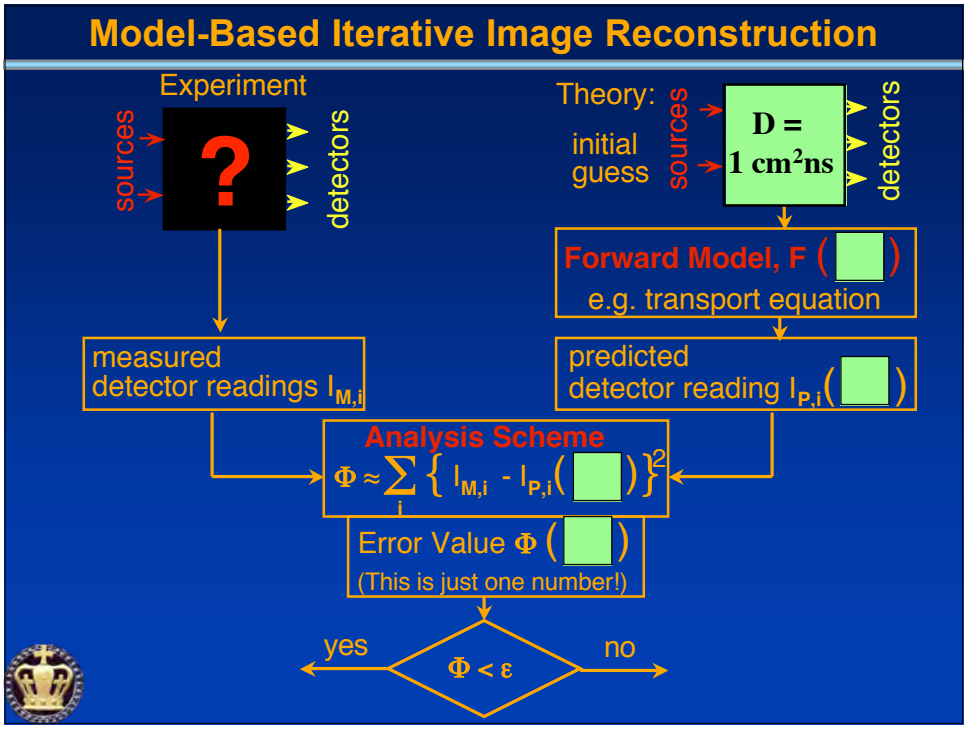
Model-Based Iterative Image Reconstruction
Experiment
sources
?
detectors
Theory:
initial guess
sources
D = 1 cm²ns
detectors
Forward Model, F ( )
e.g. transport equation
measured detector readings $I_{M,i}$
predicted detector reading $I_{P,i}$( )
Analysis Scheme
$\Phi \approx \sum_i \{ I_{M,i} - I_{P,i}( ) \}^2$
Error Value Φ ( )
(This is just one number!)
yes
Φ < ε
no

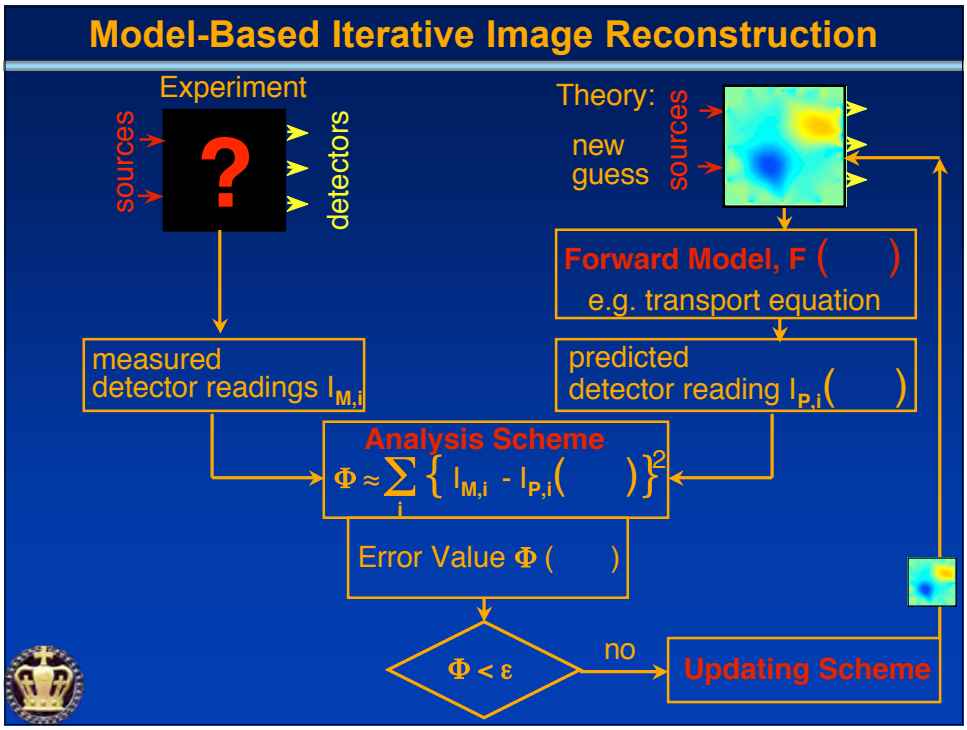
Model-Based Iterative Image Reconstruction
Experiment
sources
?
detectors
Theory:
new guess
sources
Forward Model, F ( )
e.g. transport equation
measured detector readings $I_{M,i}$
predicted detector reading $I_{P,i}$( )
Analysis Scheme
$\Phi \approx \sum_i \{ I_{M,i} - I_{P,i}( ) \}^2$
Error Value Φ ( )
Φ < ε
no
Updating Scheme

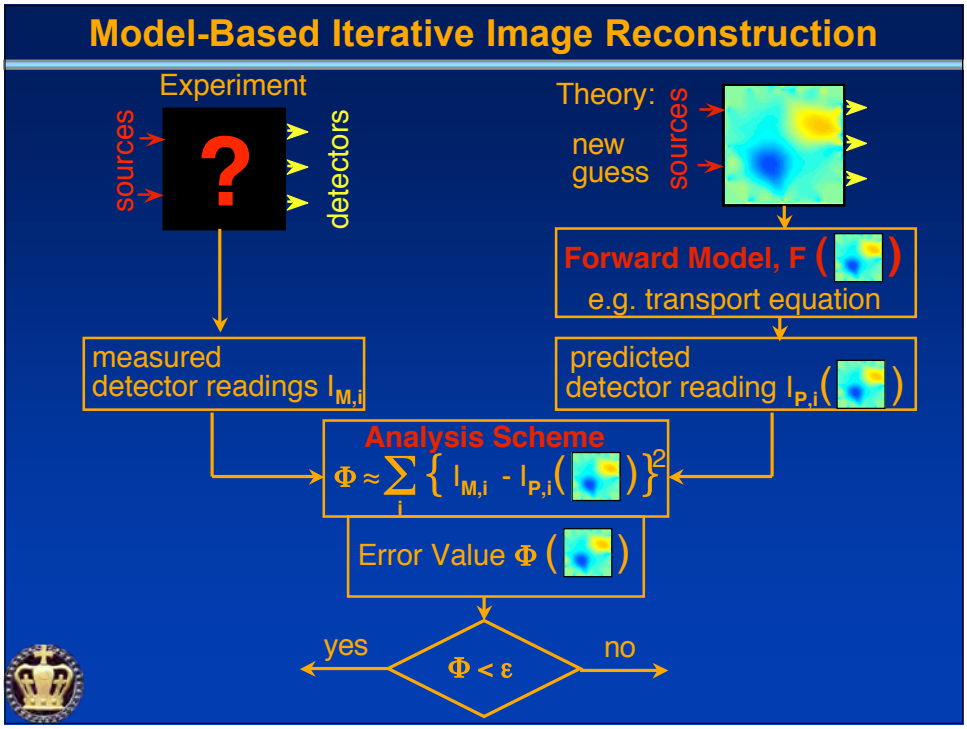
Model-Based Iterative Image Reconstruction
Experiment
sources
?
detectors
Theory:
new guess
sources
Forward Model, F ( )
e.g. transport equation
measured detector readings $I_{M,i}$
predicted detector reading $I_{P,i}$( )
Analysis Scheme
$\Phi \approx \sum_i \{ I_{M,i} - I_{P,i}( ) \}^2$
Error Value Φ ( )
yes
$\Phi < \varepsilon$
no

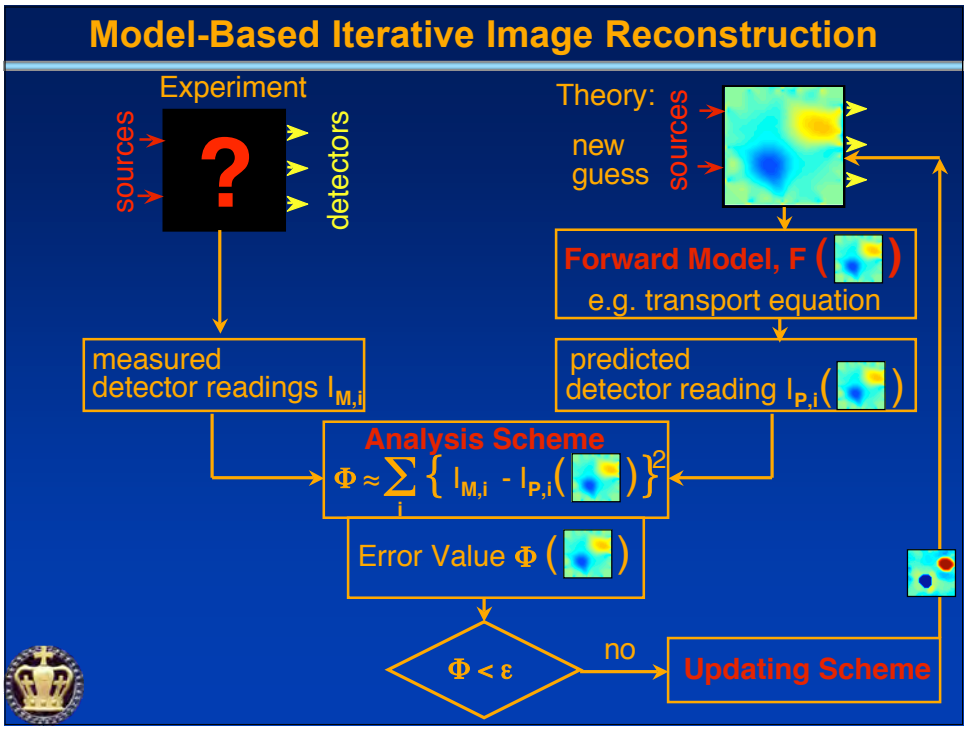
Model-Based Iterative Image Reconstruction
Experiment
sources
?
detectors
Theory:
new guess
sources
Forward Model, F ( )
e.g. transport equation
measured detector readings $I_{M,i}$
predicted detector reading $I_{P,i}$( )
Analysis Scheme
$\Phi \approx \sum_i \{ I_{M,i} - I_{P,i}( ) \}^2$
Error Value Φ ( )
$\Phi < \varepsilon$
no
Updating Scheme

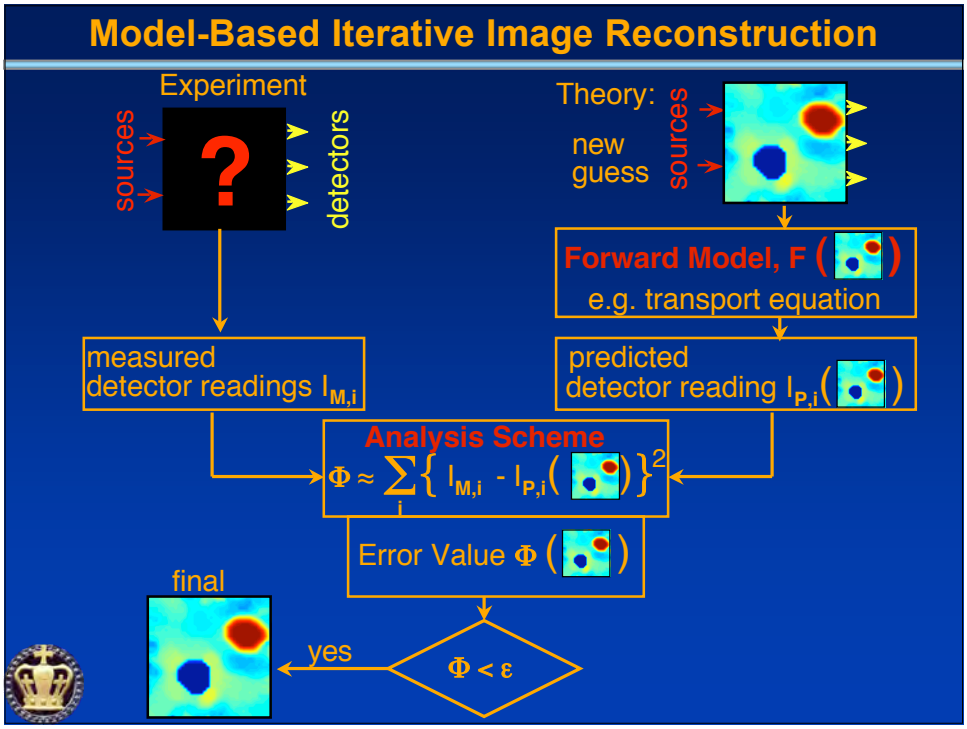
Model-Based Iterative Image Reconstruction
Experiment
sources
?
detectors
Theory:
new guess
sources
Forward Model, F ( )
e.g. transport equation
measured detector readings $I_{M,i}$
predicted detector reading $I_{P,i}$( )
Analysis Scheme
$\Phi \approx \sum_i \{ I_{M,i} - I_{P,i}( ) \}^2$
Error Value Φ ( )
final
yes
$\Phi < \varepsilon$

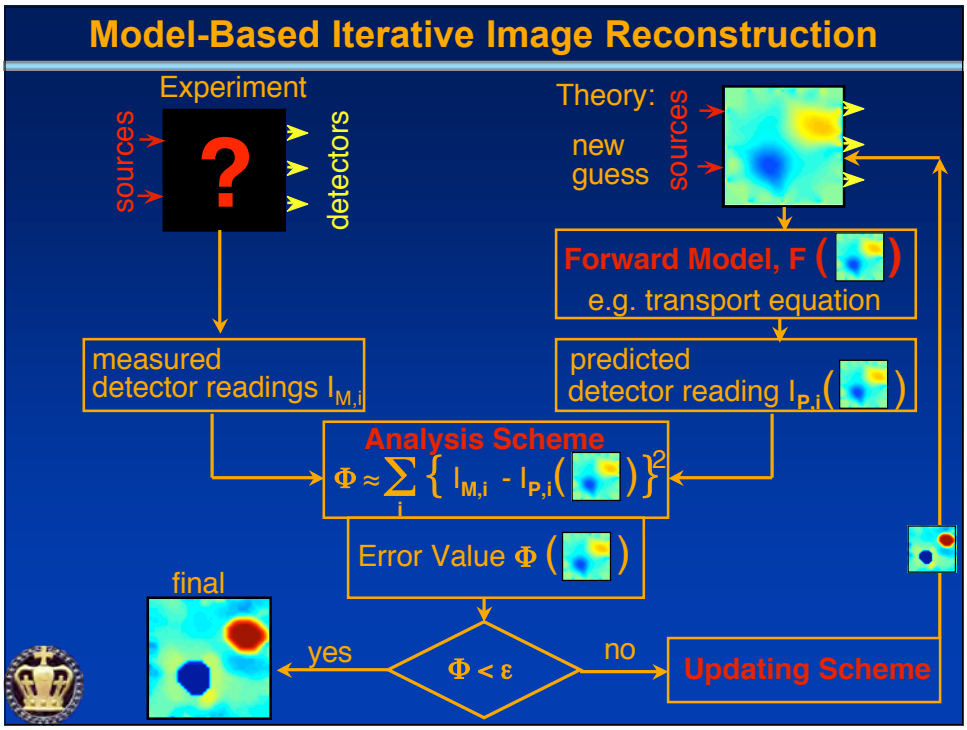
Model-Based Iterative Image Reconstruction
Experiment
sources
?
detectors
Theory:
new guess
sources
Forward Model, F ( )
e.g. transport equation
measured detector readings $I_{M,i}$
predicted detector reading $I_{P,i}$( )
Analysis Scheme
$\Phi \approx \sum_i \{ I_{M,i} - I_{P,i}( ) \}^2$
Error Value Φ ( )
final
yes
$\Phi < \varepsilon$
no
Updating Scheme

Iteration Example

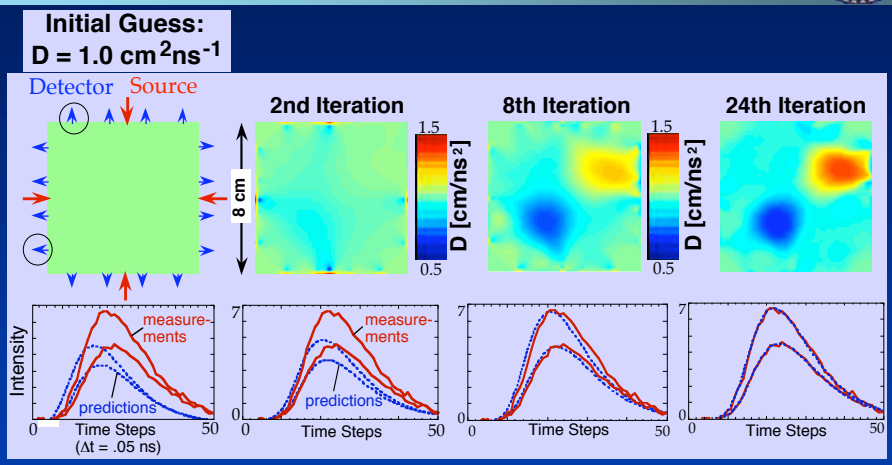

iteratively change properties of medium until measurements and predictions agree

Iterative Reconstruction

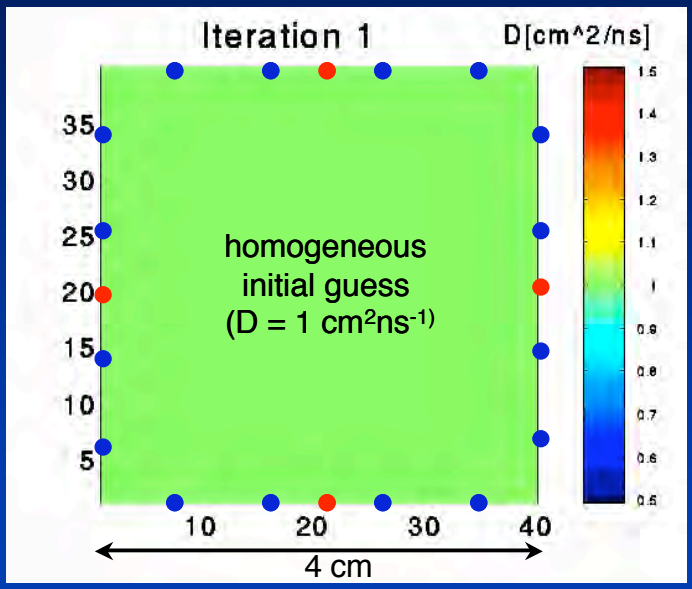

Image Reconstruction as an Optimization Problem

Find image for which error value is smallest !

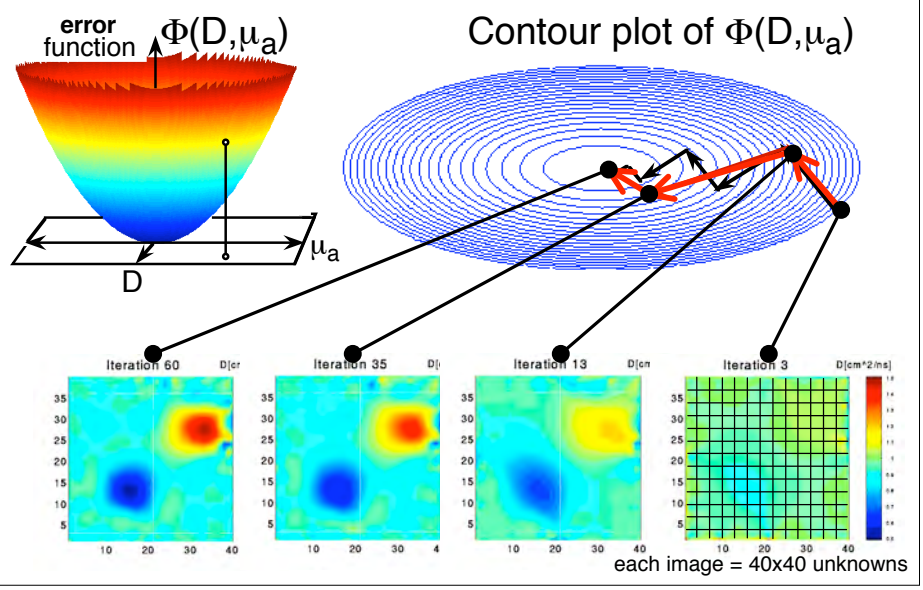

each image = 40x40 unknowns

Data Analysis Scheme

Measurement Data Y Predicted data U

$$\Phi(\mu a,D) = \sum_s \sum_d \sum_t \frac{(Y_{sdt} - U_{sdt}(\mu_a,D))^2}{2\sigma^2_{sdt}}$$

Objective Function = χ^2 Error Function

Goal : Find minimum of $\Phi(\mu a,D)$

Employ minimization technique that uses information about gradient $\frac{d\Phi(\mu a,D)}{d(\mu a,D)}$.

Gradient Calculation

Divided Difference

1 variable: 2 forward calculations needed to get gradient

$$\frac{\partial f(\zeta_x)}{\partial \zeta} = \frac{f(\zeta_2) - f(\zeta_1)}{\zeta_2 - \zeta_1}$$

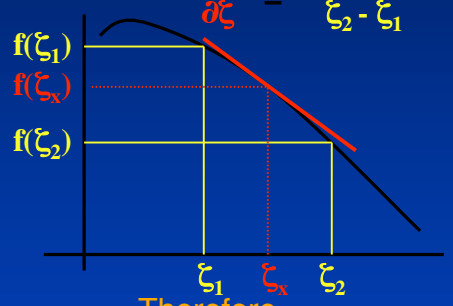

Therefore,
For problem with N unknowns one needs 2N forward calculations to find gradient.

Gradient Calculation

Divided Difference

1 variable: 2 forward calculations needed to get gradient

$$\frac{\partial f(\zeta_x)}{\partial \zeta} = \frac{f(\zeta_2) - f(\zeta_1)}{\zeta_2 - \zeta_1}$$

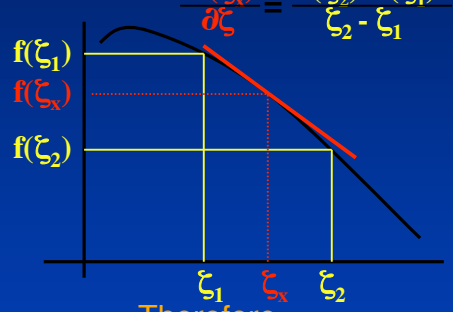

Therefore,
For problem with N unknowns one needs 2N forward calculations to find gradient.

Adjoint Differentiation

The evaluation of a gradient requires never more than five times the effort of one forward calculation!

A. Griewank, "On Automatic Differentiation," in Mathematical Programming, M. Iri, K. Tanabe, eds., Kluwer Academic Publishers, 1989, pp.83-107.

Therefore,
adjoint differentiation method is 2N/5 times faster than "traditional" divided difference scheme!

For more details see:

G. Abdoulaev, K. Ren, A.H. Hielscher, "Optical tomography as a constrained optimization problem," accepted for publication in *Inverse Problems.*

K. Ren, G. Abdoulaev, G. Bal, A.H. Hielscher, "Frequency-domain optical tomography based on the equation of radiative transfer," accepted for publication in *SIAM Journal of Scientific Computing.*

K. Ren, G. Abdoulaev, G. Bal, A.H. Hielscher, "An algorithm for solving the equation of radiative transfer in the frequency domain," *Optics Letters* 29(6), pp. 578-580 (2004).

G. Abdoulaev and A.H. Hielscher, "Three-dimensional optical tomography with the equation of radiative transfer," *Journal of Electronic Imaging* 12(4), pp. 594-60 (2003).

A.H. Hielscher, A.D. Klose, U. Netz, J. Beuthan, "Optical tomography using the time-independent equation of radiative transfer. Part 1: Forward model," *Journal of Quantitative Spectroscopy and Radiative Transfer*, Vol 72/5, pp. 691-713, 2002.

A.D. Klose, A.H. Hielscher, "Optical tomography using the time-independent equation of radiative transfer. Part 2: Inverse model," *Journal of Quantitative Spectroscopy and Radiative Transfer*, Vol 72/5, pp. 715-732, 2002.

A.D. Klose and A.H. Hielscher, "Iterative reconstruction scheme for optical tomo-graphy based on the equation of radiative transfer," *Medical Physics*, vol. 26, no. 8, pp. 1698-1707, 1999.

A.H. Hielscher, A.D. Klose, K.M. Hanson, "Gradient-based iterative image recon-struction scheme for time-resolved optical tomography," *IEEE Transactions on Medical Imaging* 18, pp. 262-271, 1999.

www.bme.columbia.edu/biophotonics

Overview

- **Introduction**
  - X-ray vs optical tomography
- **Model-based iterative image reconstruction**
  - Basic concepts and mathematical background
- **Instrumentation**
  - General optical imaging modalities
  - Dynamic optical tomography system
- **Applications**
  - Brain Imaging
  - Tumor Imaging
  - Fluorescence Imaging

Optical Imaging Modalities

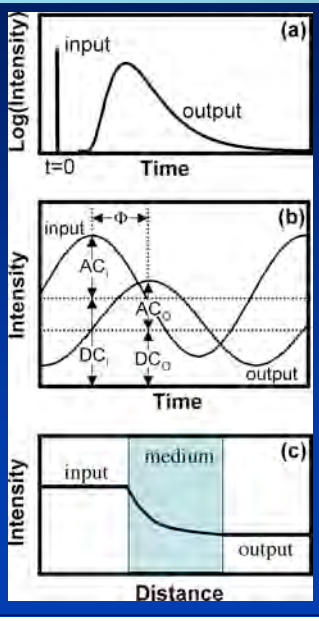

TIME DOMAIN

FREQUENCY DOMAIN

STEADY-STATE DOMAIN

information content

complexity/price of system

1 M

100k

data acquisition rate

1 image /min

10 images /sec

Frequency vs Steady-State Domain

target

steady-state domain reconstruction ($\omega = 0$)

frequency domain reconstruction (ω = 600 MHz)

absorption coefficient μ_a

scattering coefficient μ_s'

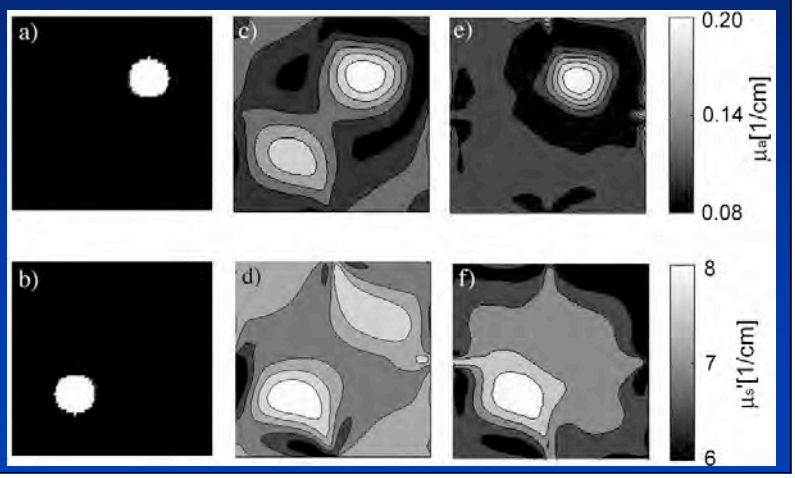

Overview

- **Introduction**
  - X-ray vs optical tomography
- **Model-based iterative image reconstruction**
  - Basic concepts and mathematical background
- **Instrumentation**
  - General optical imaging modalities
  - Dynamic optical tomography system
- **Applications**
  - Brain Imaging
  - Tumor Imaging
  - Fluorescence Imaging

Instrument Diagram

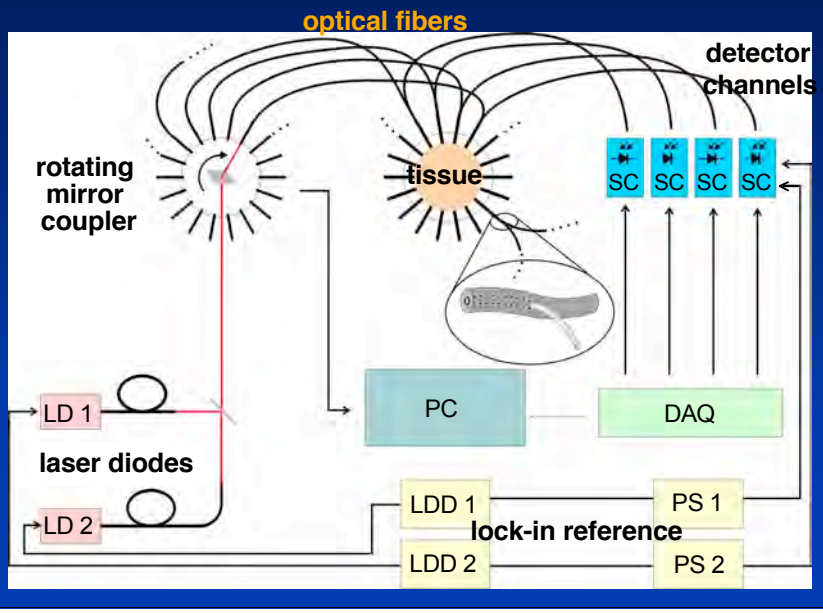

Dynamic Optical Tomography System (DYNOT)

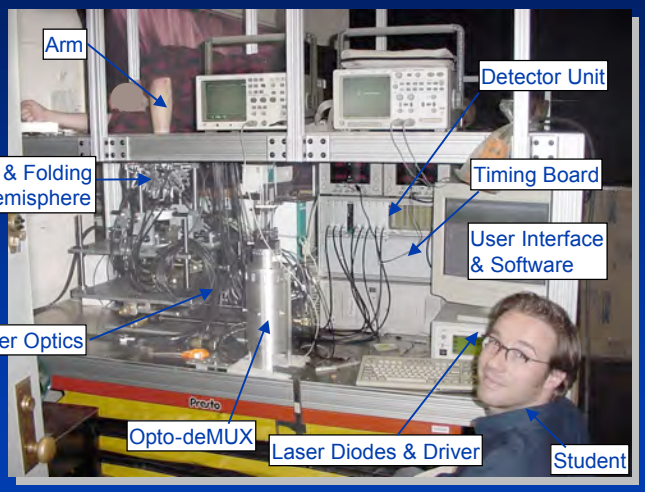

Up to 10 full tomographic images per second!

Dynamic Optical Tomography System (details)

Detector and Timing Boards

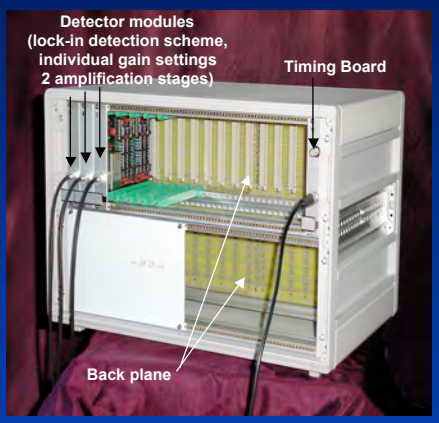

Dynamic Optical Tomography System (DYNOT)

Dynamic Range of Measurement

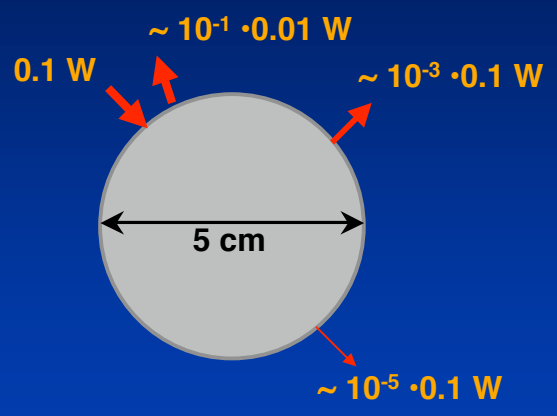

Dynamic Range of Measurement

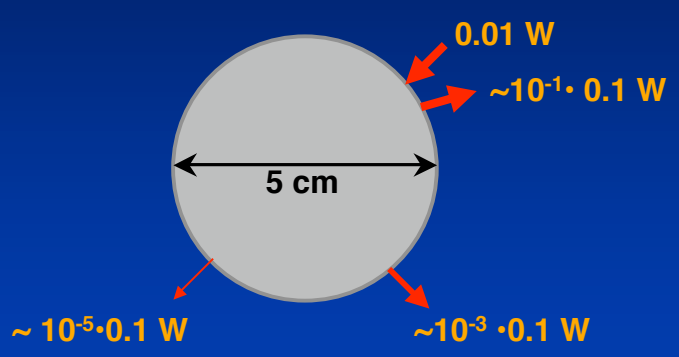

Dynamic Range of Measurement

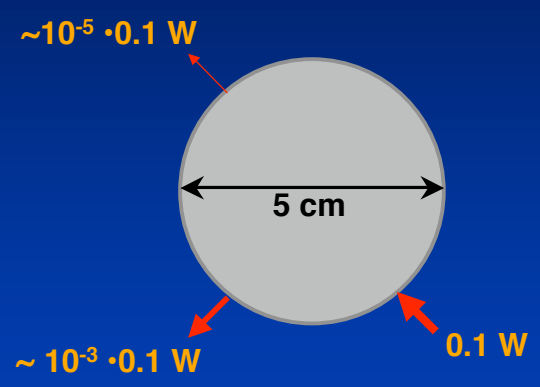

Dynamic Range of Detectors

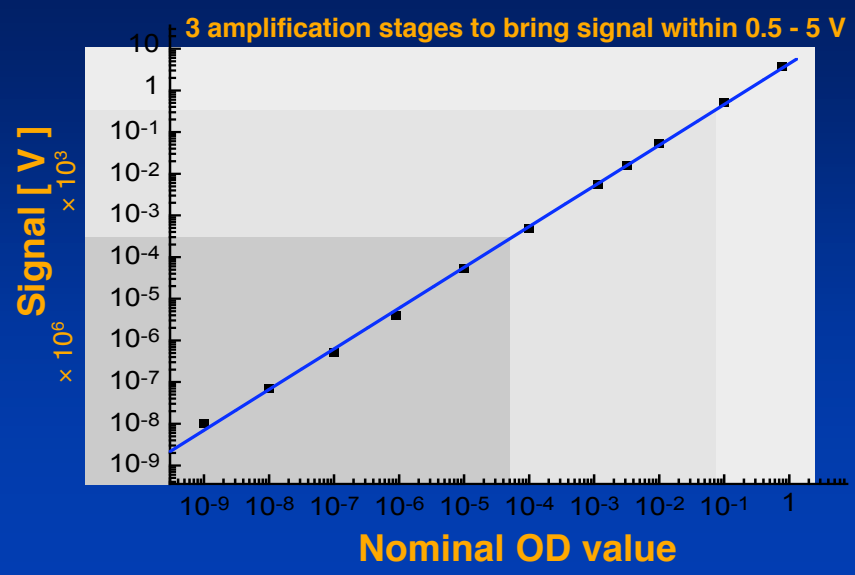

Timing Scheme

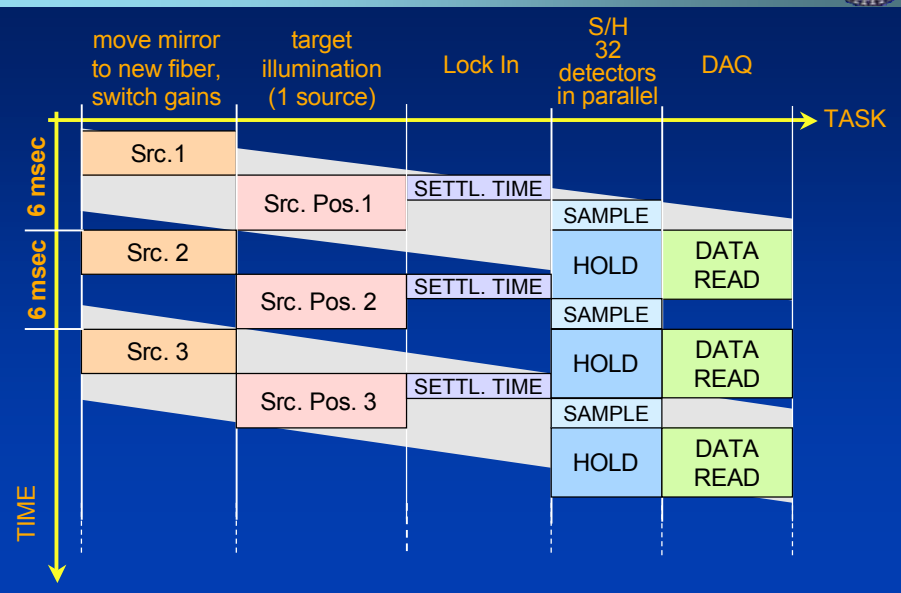

Performance Overview

Parameter	Value
Modulation frequency	5-10 kHz
Data acquisition rate	~150 Hz
Settling time	1-2 ms
Noise equivalent power	10 pW (rms)
Dynamic range	$1:10^9$ (180 dB)
Long term bias drifts	~1% over 30 min
Background light reject	~100 dB

For more details see:

A.H. Hielscher, A.Y. Bluestone, G.S.Abdoulaev, A.D. Klose, J. Lasker, M. Stewart, U. Netz, J. Beuthan, "Near-infrared diffuse optical tomography," *Disease Markers* 18(5-6), pp. 313-337 (2002).

C.H. Schmitz, M. Löcker, J.M. Lasker, A.H. Hielscher, R.L. Barbour, "Instrumentation for fast functional optical tomography," *Rev. of Scientific Instrumentation* 73(2), pp. 429-439 (2002).

C.H. Schmitz, Y. Pei, H.L. Graber, J.M. Lasker, A.H. Hielscher, R.L. Barbour, "Instrumentation for real-time dynamic optical tomography," in *Photon Migration, Optical Coherence Tomography, and Microscopy*, S. Andersson-Engels, M.F. Kaschke, eds., SPIE-The International Society for Optical Engineering, Proc. 4431, pp. 282-291, 2001.

www.bme.columbia.edu/biophotonics

Overview

- **Introduction**
  - X-ray vs optical tomography
- **Model-based iterative image reconstruction**
  - Basic concepts and mathematical background
- **Instrumentation**
  - General optical imaging modalities
  - Dynamic optical tomography system
- **Applications**
  - Brain Imaging
  - Tumor Imaging
  - Fluorescence Imaging

Animal Model

325 gm
Sprague Dawley Rats

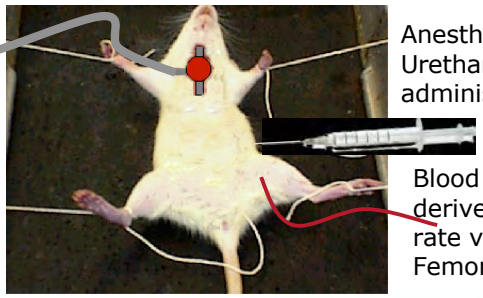

Anesthesia:
Urethane
administered *i.p.*

Ventilated at:
40-60 breaths/min
1-1.5 cc/breath

Blood Pressure and
derived respiratory
rate via
Femoral catheter

Regulate inspired
$[O_2]$ and $[CO_2]$

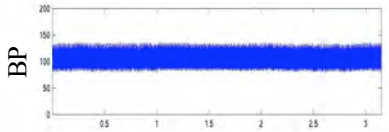

Probe Geometry

- Forehead shaven
- Animal's head fixed in place using stereotaxic
- Optical probe with fixed geometry positioned in line with lambda (λ) suture line, optodes begin 2 mm anterior to λ.

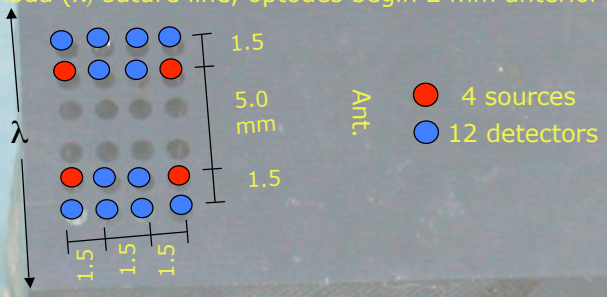

Probe Location

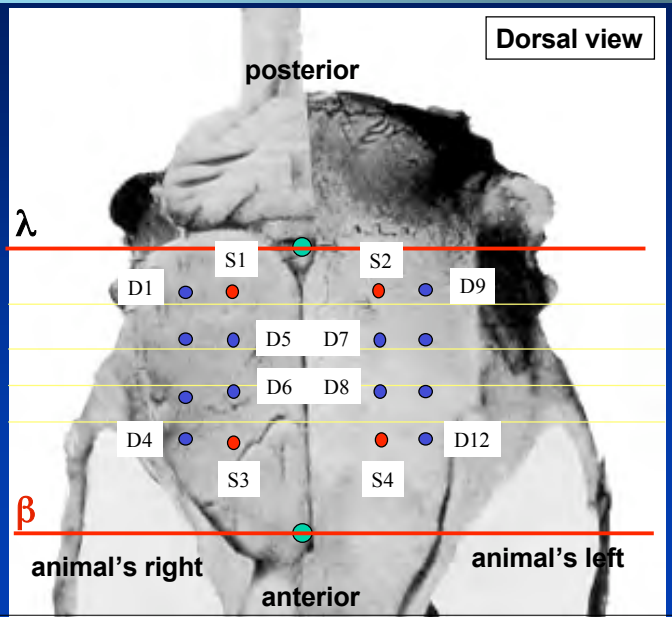

Carotid Occlusion

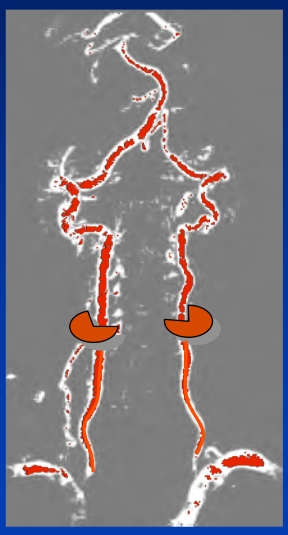

Carotid Occlusion

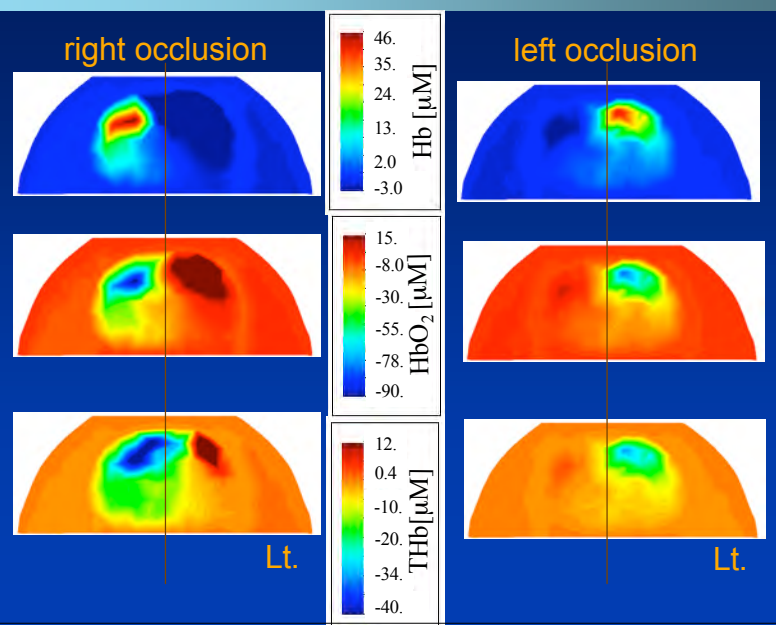

Two Wavelengths (λ_1, λ_2)

Reconstruction algorithm provides $\Delta\mu_a$ for each volume element (voxel) of finite element mesh for each wavelength.

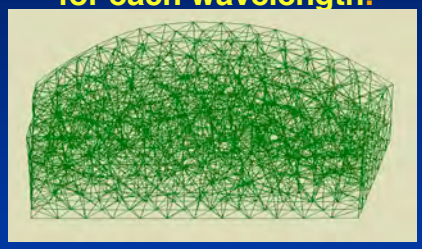

For each voxel we get two equations:

$$\Delta\mu_a^{\lambda 1} = \varepsilon_{Hb}^{\lambda 1} \quad \Delta[Hb] + \varepsilon_{HbO_2}^{\lambda 1} \quad \Delta[HbO_2]$$

$$\Delta\mu_a^{\lambda 2} = \varepsilon_{Hb}^{\lambda 2} \quad \Delta[Hb] + \varepsilon_{HbO_2}^{\lambda 2} \quad \Delta[HbO_2]$$

ε := extinction coefficient (from literature)

Two Wavelengths

Reconstruction algorithm provides $\Delta\mu_a$ for each volume element (voxel) of finite element mesh for each wavelength.

From this we can calculate changes in concentrations of oxy-hemoglobin, $\Delta[Hb]$, and dexoy-hemoglobin, $\Delta[HbO_2]$, for each voxel.

$$\Delta[Hb] = \frac{\varepsilon_{HbO_2}^{\lambda 2}\Delta\mu_a^{\lambda 1} - \varepsilon_{HbO_2}^{\lambda 1}\Delta\mu_a^{\lambda 2}}{\varepsilon_{Hb}^{\lambda 1}\ \varepsilon_{HbO_2}^{\lambda 2} - \varepsilon_{Hb}^{\lambda 2}\ \varepsilon_{HbO_2}^{\lambda 1}}$$

$$\Delta[HbO_2] = \frac{\varepsilon_{Hb}^{\lambda 1}\Delta\mu_a^{\lambda 2} - \varepsilon_{Hb}^{\lambda 2}\Delta\mu_a^{\lambda 1}}{\varepsilon_{Hb}^{\lambda 1}\ \varepsilon_{HbO_2}^{\lambda 2} - \varepsilon_{Hb}^{\lambda 2}\ \varepsilon_{HbO_2}^{\lambda 1}}$$

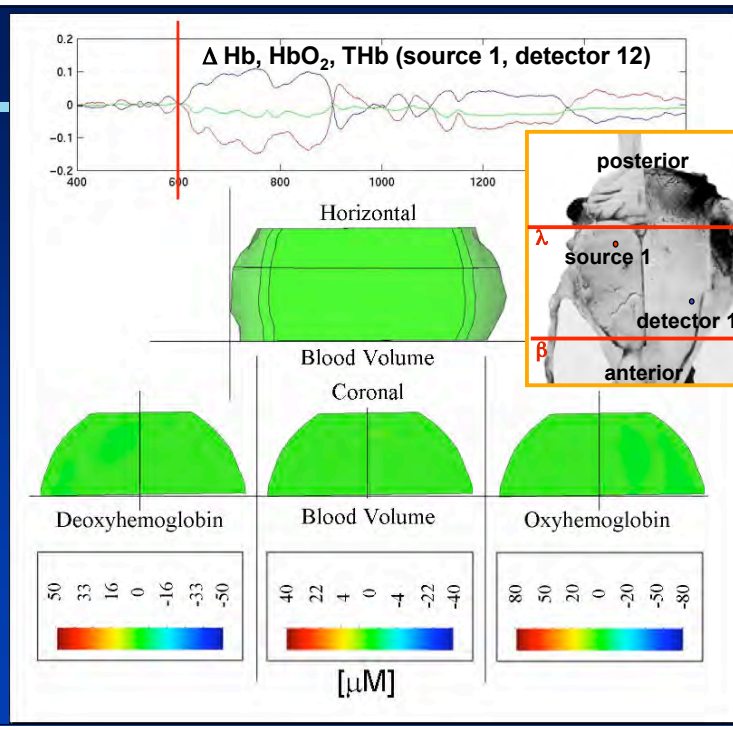

Forepaw Stimulation

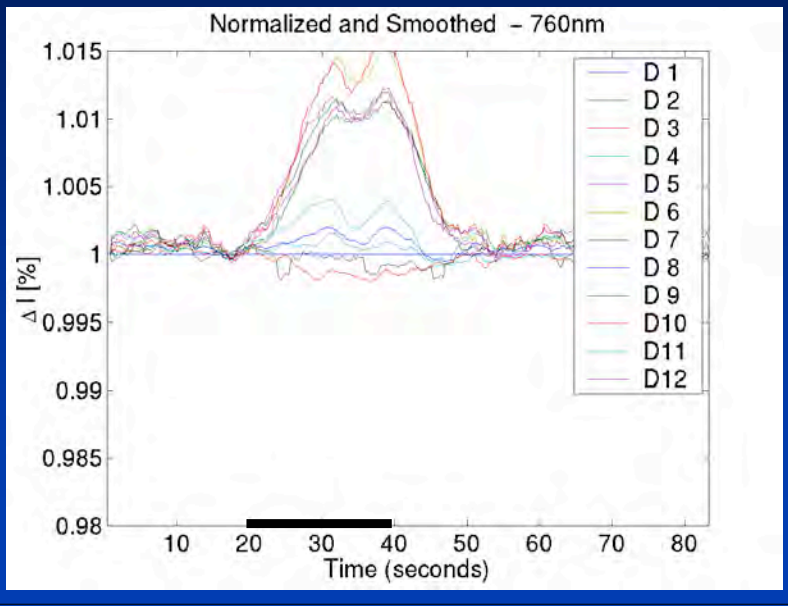

Right Forepaw Stimulation

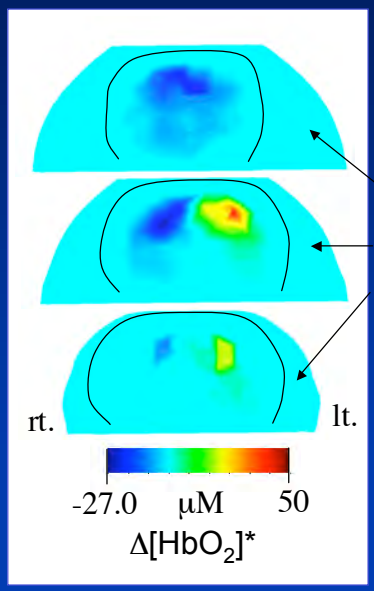

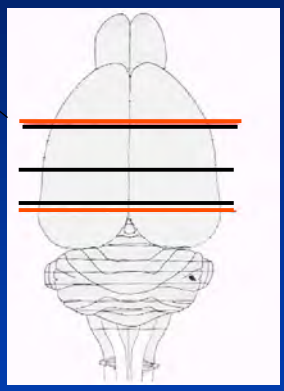

*Oxyhemoglobin

Reconstruction

Blood Volume

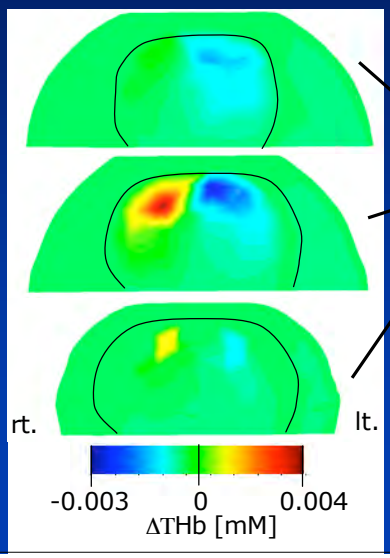

Cut 3

Cut 7

Cut 10

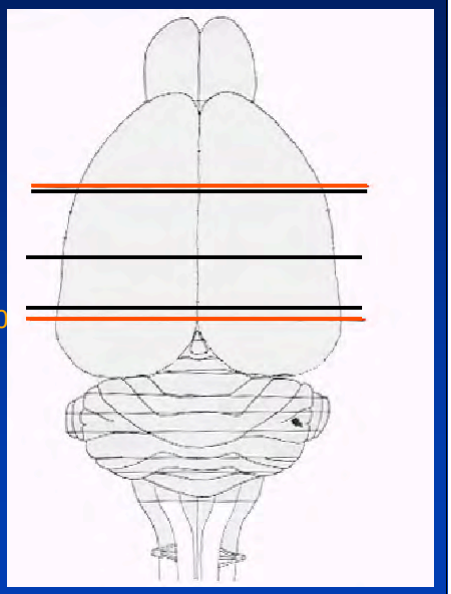

For more details see:

A.Y. Bluestone, M. Stewart, B. Lei, I.S. Kass, J. Lasker, G.S. Abdoulaev, A.H. Hielscher, "Three-dimensional optical tomographic brain imaging in small animals, Part I: Hypercapnia," *Journal of Biomedical Optics* 9(5), pp. 1046-1062 (2004).

A.Y. Bluestone, M. Stewart, J. Lasker, G.S. Abdoulaev, A.H. Hielscher, "Three-dimensional optical tomographic brain imaging in small animals, Part II: Unilateral Carotid Occlusion," *Journal of Biomedical Optics* 9(5), pp. 1063-1073 (2004).

A.Y. Bluestone, Kenichi Sakamoto, A.H. Hielscher, M. Stewart, "Three-Dimensional Optical Tomographic Brain Imaging during Kainic-Acid-Induced Seizures in Rats," in *Physiologu, Function, and Structure from Medical Images,* A. Amini, A. Manduca, eds., SPIE-The International Society for Optical Engineering, Proc. 5746, pp. 58-66 (2005).

www.bme.columbia.edu/biophotonics

Overview

- **Introduction**
  - X-ray vs optical tomography
- **Model-based iterative image reconstruction**
  - Basic concepts and mathematical background
- **Instrumentation**
  - Static Measurements
  - Dynamic Measurements
- **Applications**
  - Brain Imaging
  - Tumor Imaging
  - Fluorescence Imaging

Tumors in Mice

- **Tumor is injected into mouse left kidney.**
- **Tumor continues to grow unless treated.**
- **Treatment with VEGF antagonist seeks to stop angiogenesis and reverse tumor growth.**

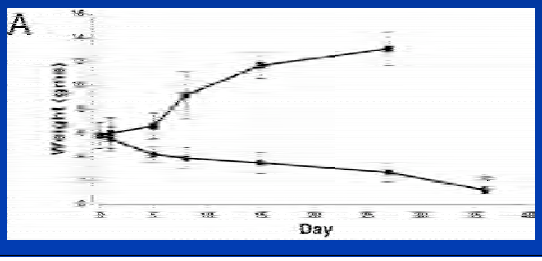

Tumors in Mice

- Untreated tumors: highly vascularized

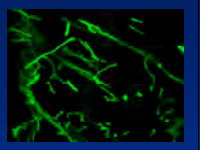

- Treated tumors: much less vascularized

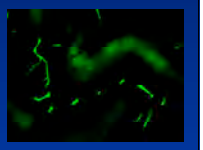

Fluorescent staining with Lectin (10 x)

- Currently:
  Many mice are sacrificed to get tumor data
- Only 1 time point per mouse
- We propose to use MRI and OT to study tumor size and vasculature in vivo

More Information:

Frischer JS, Huang JZ, Serur A, Kadenhe-Chiweshe A, McCrudden KW, O'Toole K, Holash J, Yancopoulos GD, Yamashiro DJ, Kandel JJ "Effects of potent VEGF blockade on experimental Wilms tumor and its persisting vasculature"
INTERNATIONAL JOURNAL OF ONCOLOGY 25 (3): pp. 549-553 (2004).

Huang JZ, Frischer JS, Serur A, Kadenhe A, Yokoi A, McCrudden KW, New T, O'Toole K, Zabski S, Rudge JS, Holash J, Yancopoulos GD, Yamashiro DJ, Kandel JJ "Regression of established tumors and metastases by potent vascular endothelial growth factor blockade"
PROCEEDINGS OF THE NATIONAL ACADEMY OF SCIENCES OF THE UNITED STATES OF AMERICA 100 (13): 7785-7790 (2003)

Glade-Bender J, Kandel JJ, Yamashiro DJ, "VEGF blocking therapy in the treatment of cancer"
EXPERT OPINION ON BIOLOGICAL THERAPY 3 (2): 263-276 APR 2003

fMRI vs Optical Tomography

	fMRI	Optical Tomography
Spatial Resolution	0.1mm- 1mm	2mm - 10mm
Sensitive to	Hb (paramag.)	Hb, HbO_2, cytochrome, etc, blood volume, scattering properties
Speed	0.1 - 1Hz	~50 Hz
Cost	> $500.000	~ $100.000
Portability	no	yes
Continuous Monitoring	no	yes

Combine high spatial resolution of fMRI and high speed and sensitivity of optical tomography!

9.4 Tesla MRI (Bruker Avance 400)

Micro2.5 Imaging set
35mm diameter
Linearly polarized
Birdcage coil

Typical imaging time: 30 - 60 minutes (T1 sequence)

Optical Tomography Set Up

Step 1

Lower mouse into imaging head.

Step 2

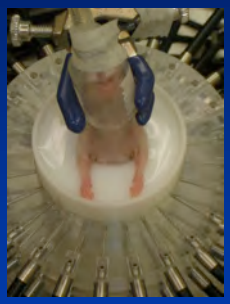

Add matching fluid (Intralipid).

Step 3

Illuminate with light (Image!)

Typical imaging time: 10 - 20 minutes

Axial Slice

Optical

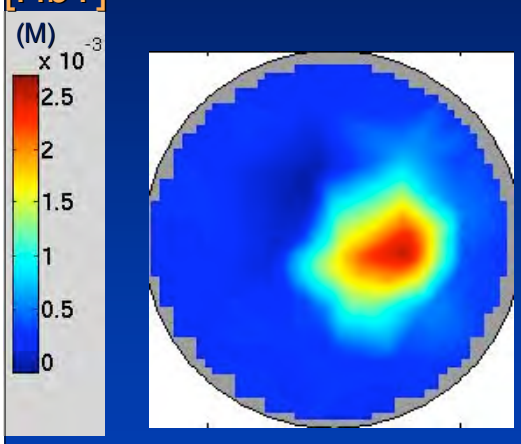

Total Hemoglobin

MRI

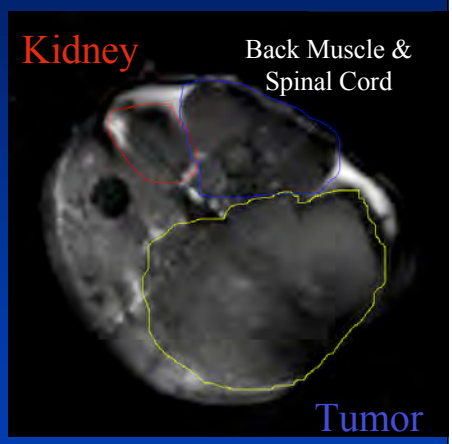

Coronal Slice

[HbT] **Optical** **MRI**

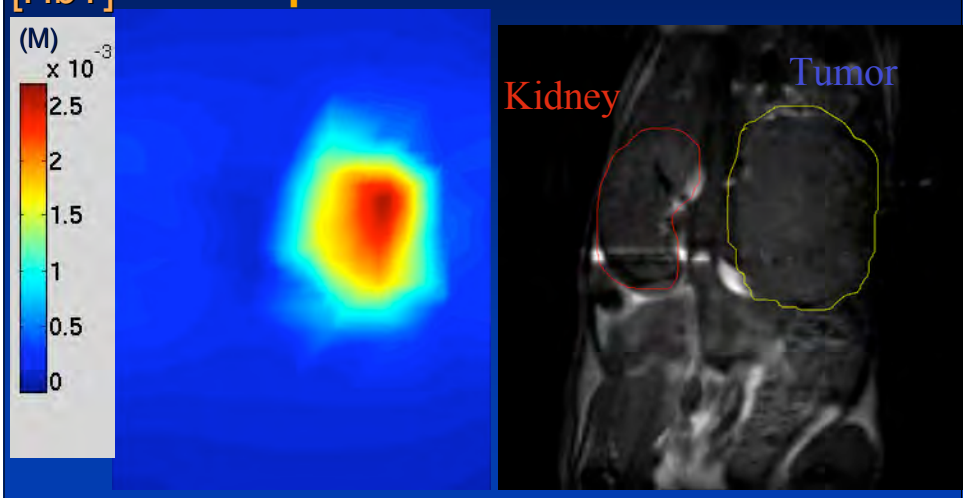

Total Hemoglobin

Compare Untreated vs. Treated

Untreated [HbT]

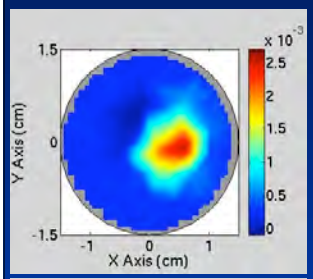

Treated [HbT]

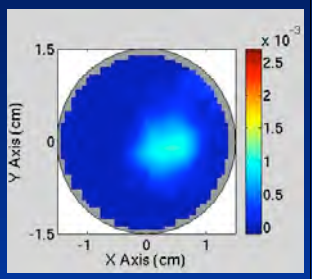

Untreated tumor has higher [HbT] than treated tumor because of higher vascularization.

Untreated tumor has higher [Hb] than treated tumor because it is HbO_2 starved.

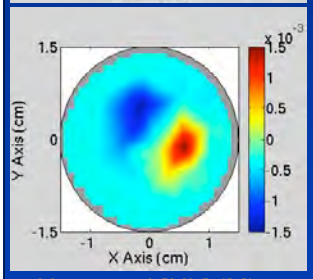

Untreated [Hb] (M)

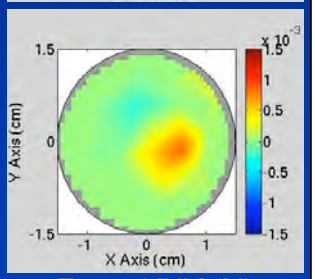

Treated [Hb] (M)

For more details see:

J. Masciotti, G. Abdoulaev, J. Hur, J. Papa, J. Bae, J. Huang, D. Yamashiro, J. Kandel, A.H. Hielscher, "Combined optical tomographic and magnetic resonance imaging of tumor bearing mice," in *Optical Tomography and Spectroscopy of Tissue VII*, B. Chance, R.R. Alfano, B.J. Tromberg, M. Tamura, E.M. Sevick-Muraca, eds., SPIE-The International Society for Optical Engineering, Proc. 5693, pp. 74-81 (2005).

www.bme.columbia.edu/biophotonics

Overview

- **Introduction**
  - X-ray vs optical tomography
- **Model-based iterative image reconstruction**
  - Basic concepts and mathematical background
- **Instrumentation**
  - General optical imaging modalities
  - Dynamic optical tomography system
- **Applications**
  - Brain Imaging
  - Tumor Imaging
  - Molecular Fluorescence Imaging

Molecular Imaging

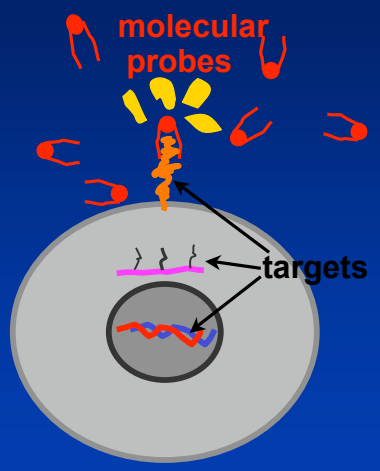

Rheumatoid Arthritis

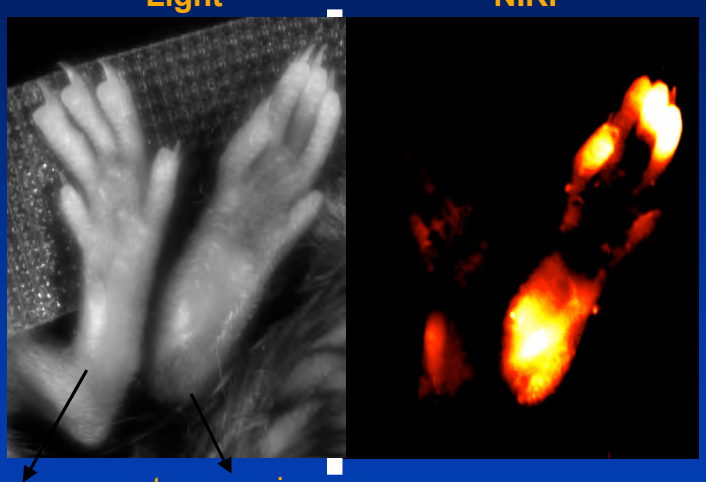

mouse
without RA

transgenic mouse
with RA

Antigen: glucose-6-phosphate isomerase (GPI)

Mahmood,
Weissleder et al
MGH-CMIR

Cancer Detection

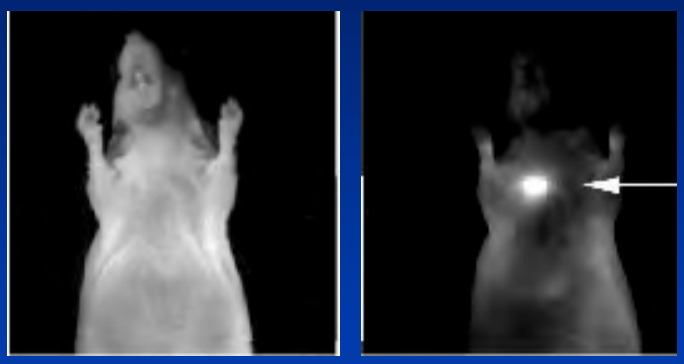

Fluorescence Tomography

reconstruction of absorption and scattering profile μ(x,y)

reconstruction of fluorescence source profile S(x,y)

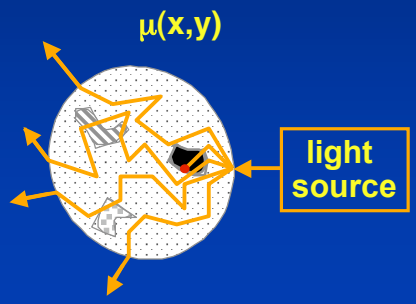

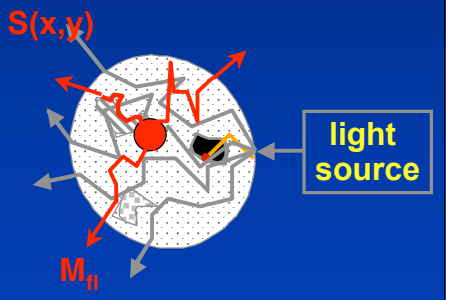

Fluorescence Tomography

1) Excitation λ^x

ϕ^x [W cm^{-2}]

$\mu_a^{x\to m}$ absorption of fluorophore

2) Emission λ^m

ϕ^m [W cm^{-2}]

η quantum yield of fluorophore

Inverse Source Problem

$$\Omega\cdot\nabla\Psi(r,\Omega)+(\mu_a+\mu_s)\Psi(r,\Omega)=S(r,\Omega)+\mu_s\int_{4\pi}p(\Omega,\Omega')\Psi(r,\Omega')d\Omega'$$

1) Excitation λ^x

$$\Omega\cdot\nabla\Psi^x+\left(\mu_a^{x\to}+\mu_a^{x\to m}+\mu_s^{x}\right)\Psi^x=S^x+\mu_s^{x}\int_{4\pi}p(\Omega,\Omega')\Psi^x(\Omega')d\Omega'$$

$$\phi^x=\int_{4\pi}\Psi^x(\Omega')d\Omega'$$

2) Emission λ^m

$$\Omega\cdot\nabla\Psi^m+\left(\mu_a^{m}+\mu_s^{m}\right)\Psi^m=\frac{1}{4\pi}\eta\mu_a^{x\to m}\phi^x+\mu_s^{m}\int_{4\pi}p(\Omega,\Omega')\Psi^m(\Omega')d\Omega'$$

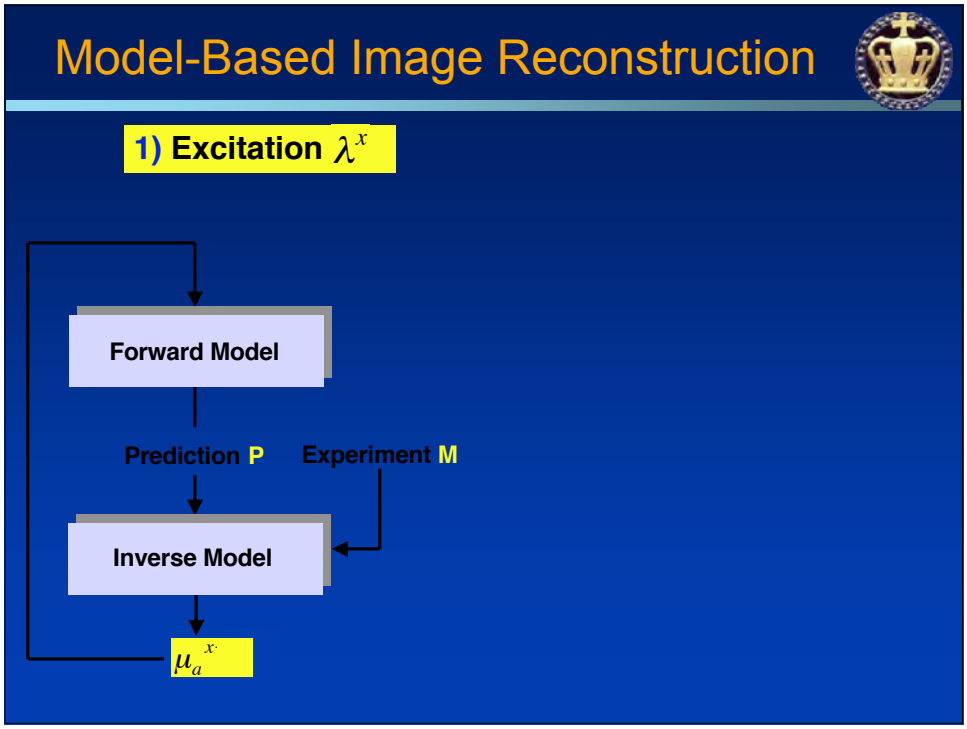
Model-Based Image Reconstruction
1) Excitation λ^x
Forward Model
Prediction P
Experiment M
Inverse Model
μ_a^x

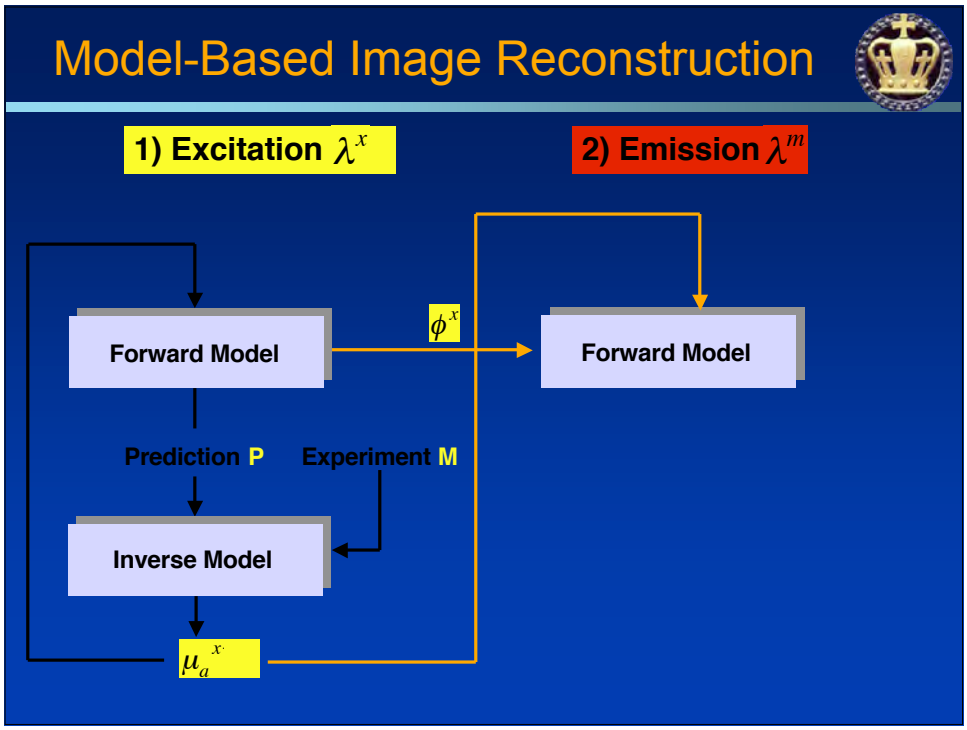
Model-Based Image Reconstruction
1) Excitation λ^x
2) Emission λ^m
Forward Model
ϕ^x
Forward Model
Prediction P
Experiment M
Inverse Model
μ_a^x

Model-Based Image Reconstruction

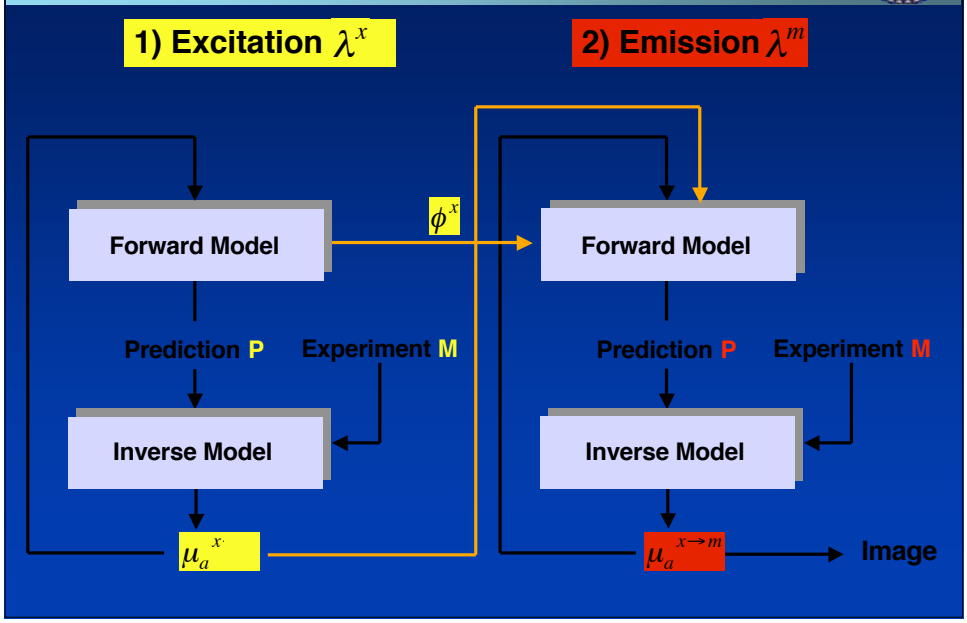

Mouse Tomography

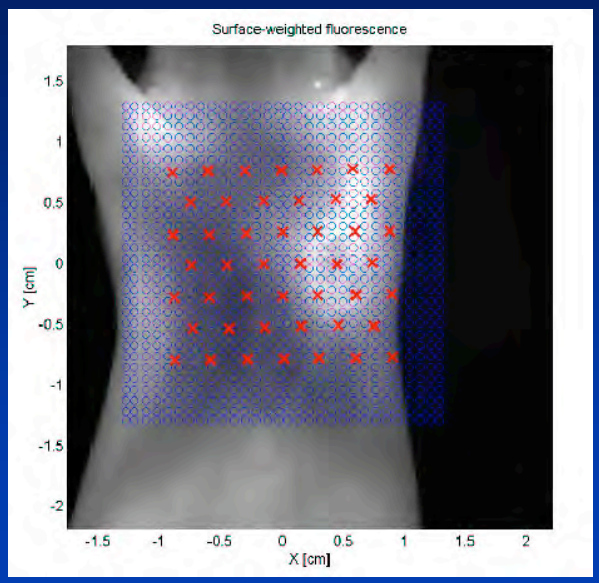

Mouse Tomography

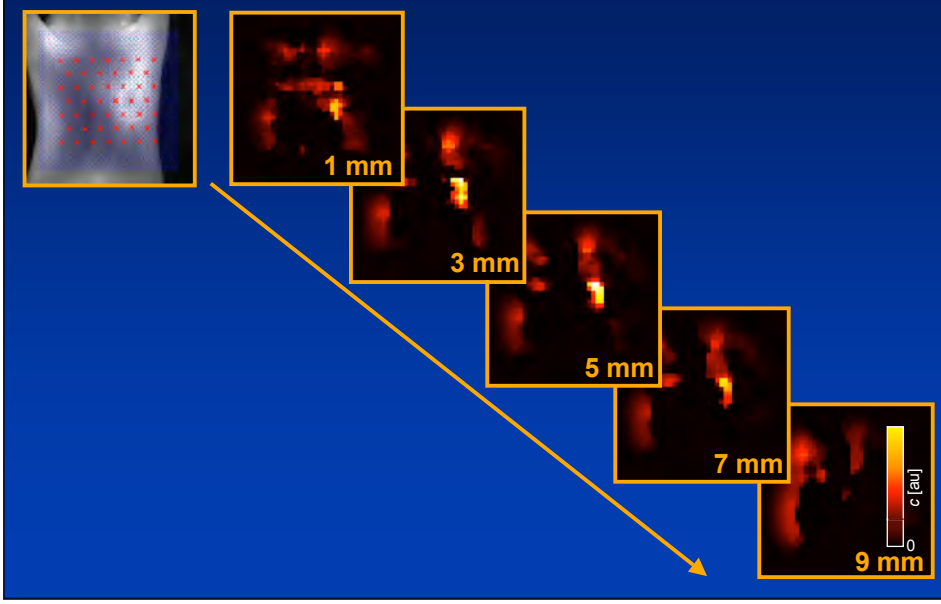

For more details see:

A.K. Klose, V. Ntziachristos, A.H. Hielscher, "The inverse source problem based on the radiative transfer equation in molecular optical imaging," *J. of Computational Physics* 202, pp. 323-345 (2005).

A.K. Klose, A.H. Hielscher, "Fluorescence tomography with the equation of radiative transfer for molecular imaging," *Optics Letters* 28(12), pp. 1019-1021 (2003).

A.K. Klose, A.H. Hielscher, " Optical fluorescence tomography with the equation of radiative transfer for molecular imaging," in *Optical Tomography and Spectroscopy of Tissue V*, B. Chance, R.R. Alfano, B.J. Tromberg, M. Tamura, E.M. Sevick-Muraca, eds., SPIE-The International Society for Optical Engineering, Proc. 4955, pp. 219-225 (2003).

www.bme.columbia.edu/biophotonics

Summary

- **Introduction**
  - X-Ray Tomography vs Optical Tomography
- **Model-based iterative image reconstruction**
  - Basic concepts and mathematical background
- **Instrumentation**
  - General optical imaging modalities
  - Dynamic optical tomography system
- **Applications**
  - Brain Imaging
  - Tumor Imaging
  - Fluorescence Imaging

Acknowledgements I

- **Students:**
  J. Masciotti, X. Gu, J. Hur, F. Provenzano, J. Lasker, A. Bluestone, B. Moa-Anderson
- **Postdoctoral Fellows:**
  A. Klose, G. Abdoulaev, J. Papa
- **Collaborators:**
  Columbia
  - J. Kandel (Pediatrics & Surgery, Columbia)
  - D. Yamashiro (Pediatrics & Surgery, Columbia)
  - G. Bal (Applied Mathematics)

  SUNY - Downstate
  - Mark Steward (Physiology & Pharmacology)
  - R.L. Barbour (Pathology)
  - C. Schmitz (NIRx Medical Technologies, Inc.)

Acknowledgements II

- National Institute of Arthritis and Musculoskeletal and Skin Diseases (NIAMS) (RO1 AR46255-01 PI: Hielscher)
- National Institute for Biomedical Imaging and Bioengineering (NIBIB) (R01 EB001900-01 PI: Hielscher and 5 R33 CA 91807-3 PI: Ntziachristos)
- National Heart, Lung, and Blood Institute (NHLBI) (SBIR 2R44-HL-61057-02)
- Whitaker Foundation (#98-0244 PI: Hielscher)
- Schering Research Foundation (PI: Klose)

More Information

COLUMBIA UNIVERSITY
IN THE CITY OF NEW YORK

www.bme.columbia.edu/biophotonics